OBSERVATION OF NEARSHORE WAVE-WAVE INTERACTION USING UAV

Yoshinao Matsuba, the University of Tokyo, matsuba@coastal.t.u-tokyo.ac.jp
Takenori Shimozono, the University of Tokyo, shimozono@coastal.t.u-tokyo.ac.jp
Yoshimitsu Tajima , the University of Tokyo, yoshitaji@coastal.t.u-tokyo.ac.jp

INTRODUCTION

Infragravity waves, generated by nearshore wave-wave interaction, potentially increase the coastal hazard. Lack of detailed observation of nearshore wave fields however makes it difficult to fully understand the behavior of infragravity waves under wave-wave interactions. These days, UAVs (Unmanned Aerial Vehicles) have enabled us to easily capture the top-view images of the dynamic nearshore behavior with sufficiently high spatial and temporal resolutions. In this study, we conducted UAV-based observations of cross-shore variations of wave spectral characteristics to clarify the nearshore wave-wave interactions.

FIELD SURVEY

The survey was conducted at Hiratsuka Coast, Japan (see Figure 1). Aerial video of the nearshore area was taken for one hour by UAVs hovering at an altitude of 150 m. Then, a timestack image was created from the video frames, from which time-varying locations of the shoreline and wave breaking points were extracted using edge detection technique as seen in Figure 2. We analyzed the spectral and bispectral characteristics of the run-up data together with wave data simultaneously obtained by two wave gauges at onshore and offshore locations.

DISCUSSION AND CONCLUSION

Figure 3 compares wave spectra at the onshore and offshore locations, and run-up spectrum. Two dominant components are found in the offshore wave spectrum: the swell component of around 0.08 Hz and the wind-wave component of 0.14 Hz. The wind-wave component is dominant over the swell component while it is significantly reduced at the onshore location probably due to wave breaking on the offshore sand bar. The run-up spectrum suggests that low frequency components (0.06 Hz and 0.02 Hz) develop through wave breaking and run-up processes. These trends can also be captured by spectral analysis of time-varying brightness at each point of UAV images. This study also applied bispectral analysis to quantify the relative intensity of nonlinear wave-wave interaction between two arbitrary wave components. Figure 4 shows the bicoherence of the three data. The nonlinear interaction is not clearly observed at the offshore location whereas strong interaction between swell and wind-wave component is confirmed at the onshore location. This result suggests that a low-frequency wave component with frequency of around 0.06 Hz was developed through this interaction because 0.06 Hz corresponds to the difference of the frequencies of wind-wave and swell components. Moreover, the interaction of the swell and the low-frequency components was also confirmed in the run-up process. The frequency difference of these components surely corresponds to the further low-frequency component (0.02 Hz) observed in the run-up spectrum (Figure 3).

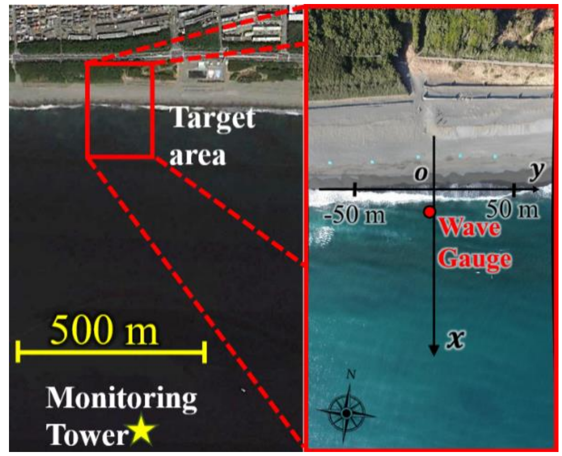

Figure 1 - Overview of the survey site and an example of the video frames taken by UAVs

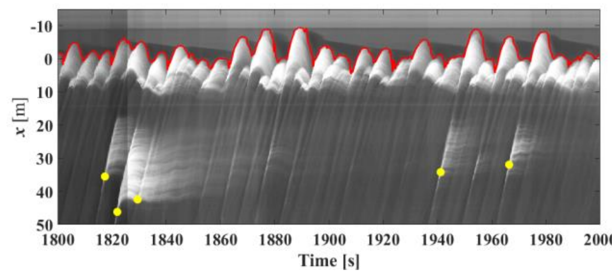

Figure 2 - Timestack image and extracted shoreline

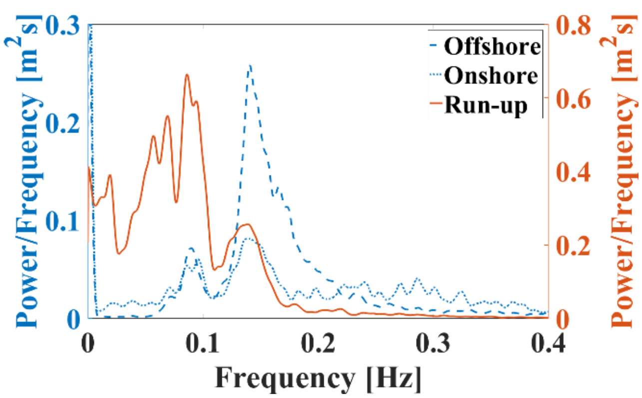

Figure 3 - The change of power spectrum density

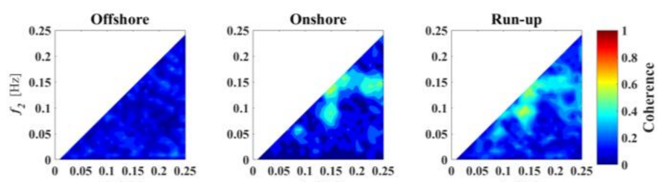

Figure 4 - Bicoherence of offshore and onshore waves and run-up